Progress in Organic Coatings 206 (2025) 109368

Contents lists available at ScienceDirect

Progress in Organic Coatings

journal homepage: www.elsevier.com/locate/porgcoat

Functionalization of 5-hydroxyindole-based i-melanin pigment for hair dyeing and UV-protective applications

Chan-Seo Yeo [a], Jongyun Choi [b], Hee-Jung Kim [c], Joo Hee Chung [c], HyunA Park [d], Jong-Bok Seo [c], Ji Chul Jung [b], Wonjong Jung [e,*], Kwon-Young Choi [a,f,**]

[a] Department of Molecular Science and Technology, Ajou University, Suwon, Gyeonggi-do, Republic of Korea
[b] Department of Chemical Engineering, Myongji University, Yongin 17058, Republic of Korea
[c] Metropolitan Seoul Center, Korea Basic Science Institute, Seongbuk-gu, Seoul 02841, Republic of Korea
[d] Biotechnology Process Engineering Center, KRIBB, Cheongju 20736, Republic of Korea
[e] Department of Mechanical, Smart, and Industrial Engineering, Gachon University, Seongnam 13120, Republic of Korea
[f] Advanced College of Bio-Convergence Engineering, Ajou University, Suwon, Gyeonggi-do, Republic of Korea

ARTICLE INFO

Keywords:
I-melanin
UV protective
Hair dyeing
Melanin coating
Antifungal activity

ABSTRACT

In this study, 5-hydroxyindole-based i-melanin was biosynthesized through enzymatic reactions catalyzed by flavin monooxygenase (FMO) and sequential MelC tyrosinase. The monomer underwent intracellular random polymerization, resulting in a novel symmetric melanin. The synthesized i-melanin exhibited a significantly darker black coloration compared to conventional melanin and demonstrated enhanced biological activities, including antioxidant and antibacterial properties. The physical and biological characteristics of i-melanin were analyzed using UV/Vis spectroscopy, ABTS assays, and growth inhibition studies. Notably, i-melanin displayed antifungal activity against *Candida albicans*. For functional applications, i-melanin was formulated as a hair dye and incorporated into a UV-protection cream through complexation with ZnO. Both formulations exhibited excellent dyeing efficacy and UV-blocking performance. Given the high production yield of i-melanin, its scalability for industrial applications appears promising. These findings suggest that this novel melanin has potential for integration into various functional products in the future.

1. Introduction

Melanin pigments are black-to-brown pigments found in various forms in nature [1–3]. Depending on the method of synthesis and substrate, melanin exists in different forms, such as eumelanin, pyomelanin, allomelanin, pheomelanin, and neuromelanin [1,4–7]. Each type of melanin exhibits distinct colors and physicochemical properties based on its structural characteristics. Eumelanin, the most well-known form, is synthesized using L-tyrosine as a substrate through enzymatic reactions involving tyrosinase [8]. In contrast, pyomelanin is synthesized from the same substrate, L-tyrosine, via reactions catalyzed by the HPPD enzyme [9].

In the human body, melanin serves as the primary pigment responsible for forming black pigmentation in hair, eyes, and skin [10]. It is recognized as an essential pigment that protects cellular nuclei from external UV radiation. Additionally, it is known to possess various physiological activities, including body temperature regulation through its high thermal conductivity [11]. Owing to these functional properties, melanin pigments have been investigated for various applications as functional materials, particularly as UV-protective agents, as well as dyeing and coating materials [2,12–16].

Microbial-derived melanin, in particular, has been produced through microbial cultivation and utilized as a bioactive material due to its antibacterial, antioxidant, and UV-protective properties. Recently, strains capable of simultaneously producing polyhydroxybutyrate (PHB) biodegradable polymers and eumelanin were developed [17,18]. These studies demonstrated that the incorporation of eumelanin into PHB enhances the antioxidant and antibacterial properties of the polymer while improving its thermal stability [18]. Additionally, research has been reported on the incorporation of melanin into hydrogels for use in adhesive sensors [19]. Beyond its biological activities, thermally treated melanin has also been applied in materials requiring high thermal

* Corresponding author.
** Correspondence to: K.-Y. Choi, Advanced College of Bio-Convergence Engineering, Ajou University, Suwon, Gyeonggi-do, Republic of Korea.
E-mail addresses: wonjongjung@gachon.ac.kr (W. Jung), kychoi@ajou.ac.kr (K.-Y. Choi).

https://doi.org/10.1016/j.porgcoat.2025.109368
Received 2 March 2025; Received in revised form 28 April 2025; Accepted 5 May 2025
Available online 12 May 2025

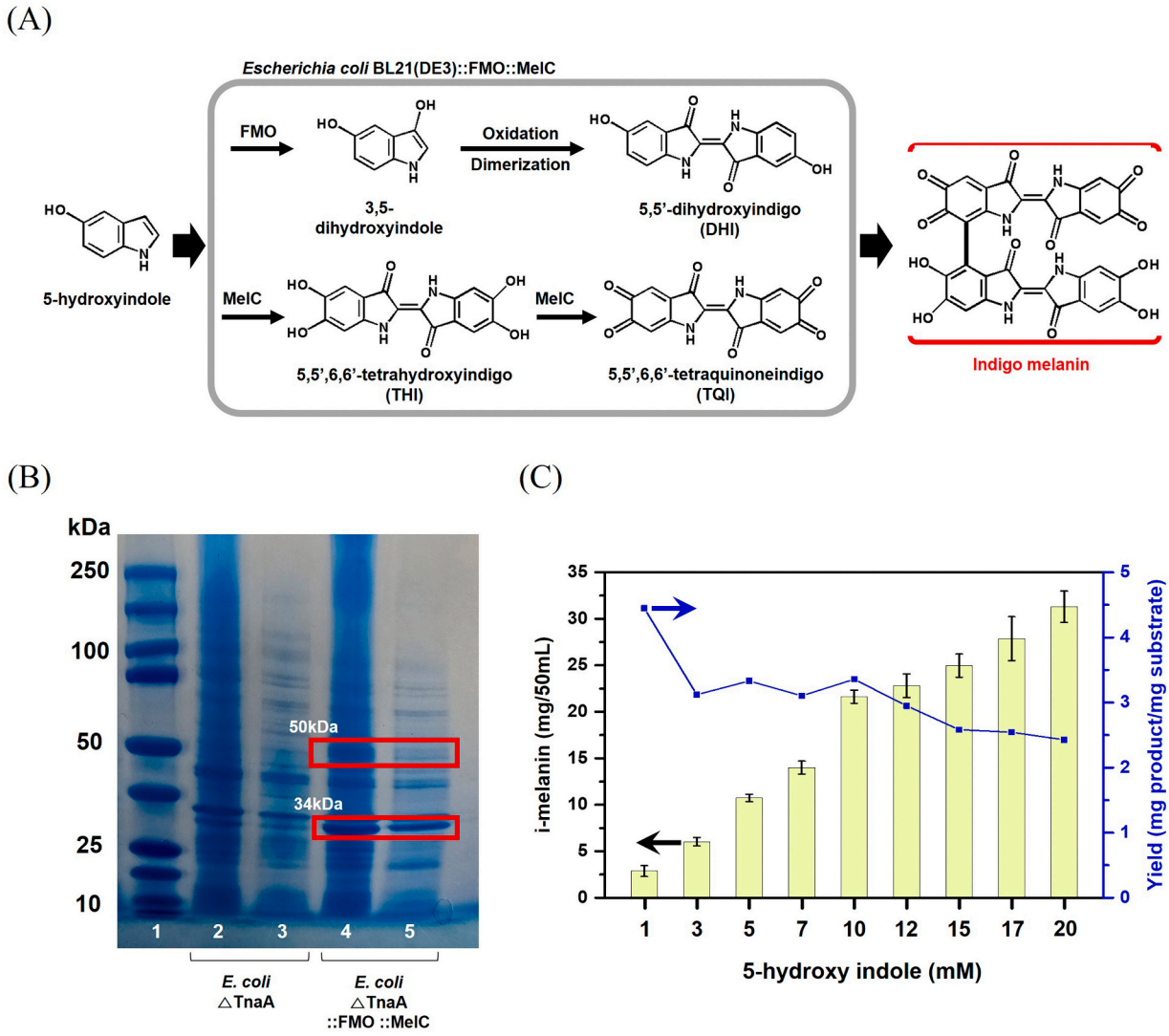

Fig. 1. (A) Synthetic scheme of i-melanin inspired by the indigo biosynthetic pathway, utilizing 5-hydroxyindole as a substrate for C3 hydroxylation. (B) Expression of FMO and MelC proteins in *Escherichia coli*, with analysis by SDS-PAGE. (C) Production of i-melanin as a function of varying 5-hydroxyindole substrate concentrations. The insert line indicates the yields of i-melanin by mg melanin/mg substrate.

stability and electrical properties, such as battery components and electrical resistance sensors [12,19,20]. Additionally, melanin pigments derived from marine organisms, along with their metal oxide forms, have been reported to offer versatile applications in industrial biomaterials, including antifouling coatings and biofouling treatment materials [21–24].

Despite the diverse functionality and applicability of melanin, its biosynthesis process presents limitations due to radical-based random polymerization, which contributes to its structural complexity. In eumelanin synthesis, various monomers, including dihydroxyindole, indole-5,6-quinone, dihydroxyindole carboxylic acid (DHICA), and indole-5,6-quinone carboxylic acid, serve as building blocks in a randomly polymerized network [25,26]. Similarly, the biosynthesis of allomelanin and pyomelanin involves the polymerization of diverse monomers, making it challenging to identify well-defined structures within melanin [26]. This structural characteristic is analogous to the random polymerization observed in lignin, a biopolymer that reinforces cellulose and hemicellulose [27]. In lignin synthesis, monomers such as *p*-coumaryl alcohol, coniferyl alcohol, and sinapyl alcohol contribute to its complex polymeric structure [27,28].

Although defining the precise structure of melanin remains a significant challenge, controlling monomer composition during its biosynthesis has emerged as a promising strategy for tailoring its functional properties. For example, melanin, which is typically insoluble, can achieve enhanced solubility through the incorporation of water-soluble monomers [19]. Furthermore, introducing specific functional groups to monomers allows for a degree of structural order within the otherwise random polymerization process [12,29–31].

Previously, we reported an indigo synthesis-inspired approach to i-melanin production, leveraging the biosynthetic pathway of indigo pigments to introduce a symmetric melanin structure. Indigo, a blue pigment derived from tryptophan, is synthesized through hydroxylation at the C3 position, followed by oxidation and symmetric dimerization of radicals at the C2 position [31]. With a long history of use as a plant-derived dye, indigo is widely recognized for its application in denim dyeing. Enzymes such as flavin monooxygenase (FMO), toluene monooxygenase (TMO), and cytochrome P450 (CYP) have been identified as key catalysts in the biosynthesis of indigo [32–37]. Notably, in this pathway, indole serves as the substrate for dimerization, exhibiting structural similarity to dihydroxyindole (DHI), which functions as the primary monomer in eumelanin biosynthesis from tyrosine.

Based on this structural resemblance, we developed a strategy to synthesize symmetric hydroxyindigo using FMO-catalyzed reactions with 5-hydroxyindole as the substrate [12,40]. This was followed by

MelC tyrosinase-mediated polymerization to generate symmetric melanin complexes (Fig. 1A) [12]. To enable the biosynthesis of these compounds, an *E. coli* strain was engineered, and the resulting indigo-like melanin was designated as i-melanin [12,40]. Additionally, i-melanin could be synthesized using L-tyrosine as a substrate, which serves as a starting material for eumelanin synthesis. The resulting i-melanin exhibited electrical conductivity and had potential applications in thin-film transistors [12,40]. However, eumelanin byproducts formed during i-melanin synthesis, as well as radical-generating intermediates such as DHICA, may interfere with the desired polymerization of i-melanin. Furthermore, the additional supply of heme precursors required for CYP102G4 enzyme activation could be limited [12,40].

Remarkably, i-melanin exhibited a significantly darker black coloration than conventional eumelanin and pyomelanin, suggesting enhanced UV-protection properties. To explore its functional applications, biosynthesized i-melanin was incorporated into formulations for hair dye and UV-protection creams. This study successfully demonstrates the synthesis of a novel melanin variant with excellent dyeing and UV-blocking capabilities. Furthermore, these findings highlight the potential for expanding melanin applications as a functional material across various fields. Additionally, this research provides insights into tailoring melanin functionalities through structural modifications of substrates or monomers involved in random polymerization.

2. Materials and methods

2.1. Chemicals and reagents

5-Hydroxyindole and 2,2′-azino-bis(3-ethylbenzothiazoline-6-sulfonic acid) (ABTS), copper sulfate, hydrogen peroxide were acquired from Sigma-Aldrich (Suwon, Gyeonggi-do, South Korea). Acetone, chloroform, methyl alcohol, ethyl alcohol, sodium bicarbonate, sodium carbonate, sodium hydroxide, ethyl acetate, and dimethyl sulfoxide were of analytical grade or higher and were purchased from Daejung (Seoul, South Korea). Additionally, Luria Bertani (LB) medium, nutrient broth (NB), and Muller-Hinton broth were obtained from Difco (Seoul, South Korea). Tris-Glycine-PAG.SDS precast gel (12 %), Tris-Glycine SDS running buffer, and Protein Ark Quick Coomassie stain were purchased from KOMA Biotech (Seoul, South Korea).

2.2. Bacterial species and cultivation conditions

The gene sequence of MelC tyrosinase was obtained from *Bacillus megaterium* ATCC 10778 and cloned into a pACYC184 vector. The gene sequence of MaFMO was obtained from *Methylophaga aminisulfidivorans* and cloned into a pET-28a(+) expression vector [36]. These genes were transformed into the host strain, *E. coli* BL21 (DE3), which was used as the host.

2.3. Expression of FMO and MelC enzyme and whole cell biotransformation of 5-hydroxyindole

To prepare the inoculum, the host strain was inoculated into LB broth and incubated with shaking at 200 rpm at 37 °C overnight. Following this, 1 % (*v*/v) of the culture medium was transferred into fresh LB medium and further incubated at 200 rpm at 37 °C until OD_{600} reached approximately 0.6–0.7. Subsequently, 0.25 mM IPTG as an inducer was added to the medium. The culture temperature was then lowered to 30 °C and maintained overnight. To analyze the expressed protein, the culture was centrifuged at 4 °C at 8000 rpm for 10 min, and the supernatant was discarded. The remaining cell pellet was washed twice with 0.1 M Tris-HCl buffer (pH 7.5) and resuspended in the same buffer to reach an OD_{600} of 10.

Cell lysis was performed by sonication, and each sample was mixed with an equal volume of DTT, then heated at 100 °C for 5 min to denature the proteins. Protein samples were loaded onto an SDS gel and subjected to electrophoresis at 120 V for 100 min using SDS running buffer. The gel was then stained with Coomassie stain solution for 15 min and destained with distilled water for at least 6 h. For whole cell biotransformation of 5-hydroxyindole, it was added to the cell culture to the final concentration of 10 mM. Whole cell production proceeded at 30 °C for 24 h in a high-speed incubator (200 rpm).

2.4. Melanin extraction, quantification and solubility test

The synthesized i-melanin was purified from the biotransformation medium by centrifugation at 4 °C at 8000 rpm for 10 min. To precipitate and isolate synthetic melanin, the supernatant obtained after centrifugation was transferred to a new bottle, and its pH was adjusted to 2.0 by adding 6 M HCl. After 4 h of incubation at 25 °C, the precipitated I-melanin was collected by centrifugation at 8000 rpm for 15 min. The isolated I- melanin pellets were washed three times with distilled water. Washed I- melanin powder was obtained by drying at 60 °C for 24 h.

For quantitative analysis of the i-melanins, HPLC and spectrometric analysis were used [5,18,19,38]. The HPLC was equipped with a UV detector and reverse phase column C18 column (Zorbax extend —C18 Waters, 250 nm × 4.6 nm, 3.5 μm, Agilent, USA). A gradient scheme of solvent A (0.1 % TFA in water) and solvent B (0.1 % TFA in acetonitrile) were applied. The ratio of A and B was 7:3. The temperature of the column was 30 °C. The absorbance of the eluent was monitored at 254 nm. The flow rate was 1 mL/min. The collected I- melanin powder was divided into 1 mg portions and dissolved in various solvents, and their optical density was measured for comparison. (+++: very well dissolved / ++: well dissolved / +: partially dissolved / -: not dissolved).

2.5. Separation and structural analysis of i-melanin by MADL-TOF analysis

The melanin sample was analyzed using an ASTA IDSys MALDI-TOF mass spectrometer (ASTA, Suwon-si, South Korea) equipped with a high-resolution camera and Yb:YAG UV laser. The powdered samples and the MS calibration standard (Liq (C_9H_6NOLi)) were prepared by depositing them onto carbon tape (Teroka Tape, thickness: 0.02 mm). Laser desorption/ionization (LDI)-TOF-MS was employed as the data acquisition method. The analysis was conducted with a laser having the following specifications: wavelength of 343 nm, pulse width of 1 ns, 1 kHz repetition rate of 1000 Hz, 55 % output, and 250 laser shots. MS spectra were visualized using IDSys analysis software (ver. 2.0.7).

2.6. Spectral feature and physical properties of i-melanin by UV spectrometer, SEM, TGA

The characteristic and structural properties of synthetic melanin were analyzed. UV/Vis spectrometry was conducted using an Epoch Microplate Spectrophotometer (BioTek, Seoul, Korea)). For surface analysis of i-melanin and quantitative analysis of surface elements, field emission SEM (FE-SEM) and energy dispersive x-ray spectrometry (EDS) were performed using the JSM-7900F (JEOL, Seoul, Korea). The morphological properties of I- melanin were assessed by SEM at an accelerating voltage of 5 kV. Thermogravimetric analysis (TGA) was conducted using the Discovery TGA 5500 (Waters, Seoul, Korea). For surface analysis of i-melanin, field emission SEM (FE-SEM) was performed using the JSM-7900F (JEOL, Seoul, Korea). The morphological properties of I- melanin were assessed by SEM at an accelerating voltage of 5 kV. Thermogravimetric analysis (TGA) was conducted using the Discovery TGA 5500 (Waters, Seoul, Korea).

2.7. Determination of radical scavenging capacity of i-melanin by ABTS assay

To assess the antioxidant capacity of I- melanin, the ABTS antioxidant assay was performed by measuring its radical scavenging ability

[5,18]. The reaction solution (14.8 mM ABTS solution dissolved in PBS and 4.9 mM potassium persulfate solution) was prepared by adjusting the pH to 7.4. After incubation for 24 h in the dark, the reaction mixture was diluted to achieve an OD at 734 nm of approximately 0.7. The absorbance of the final solution was then measured at 734 nm. Finally, the ABTS scavenging capacity was calculated using the following formula:

$$Antioxidant\ activity\ (AA\%) = \left[\frac{A_{control} - A_{sample}}{A_{control}}\right] \times 100$$

2.8. Determination of antibacterial activity of i-melanin

Candida albicans (KCTC 7965) and *Escherichia coli* (KCTC 2571) were used for the antibacterial test [5,18]. To prepare the inoculum, the strains were inoculated into NB and LB broths, respectively, and incubated with shaking at 200 rpm at 37 °C overnight. Following this, 1 % (*v*/v) of the culture medium was transferred into fresh Mueller-Hinton Broth, with 1 mg/mL of I- melanin added simultaneously. The absorbance at OD 600 was measured to determine the initial (0-h) optical density, and the cultures were further incubated at 200 rpm at 37 °C. After 18 h, the absorbance at OD 600 was measured to calculate growth inhibition. To account for the color of melanin, a control medium with only 1 mg/mL sterilized melanin was prepared, and its absorbance was measured to adjust for background absorbance

$$Growth\ inhibition\ effect(\%) = \left[\frac{OD_{600,0h} - OD_{600,18h}}{OD_{600,0h}}\right] \times 100$$

2.9. Determination of electrical conductivity of i-melanin

I- melanin was heat-treated at 800 °C for 1 h under N_2 gas. The heat-treated melanin was then mixed with a conductive additive and binder in a ratio of 9:1:1 at 400 rpm for 2 h. Super P was used as the conductive additive, and PVDF solution served as the binder. Following this, coating was applied to an OHB film at various thicknesses, and to evaporate NMP (N-Methyl-2-pyrrolidone), the solvent of the binder, the coated film was dried in a 70 °C oven. The resistance was then measured using a four-point probe. The four-point probe measurement was performed with a CMT SR2000n (AiT Co., Ltd., Suwon, Gyeonggi-do, South Korea). The electrical conductivity was calculated using the following formula.

$$Conductivity(S/cm) = \frac{1}{Resistivity}, Resistivity(\Omega \bullet cm) = \Omega \Big/ sq \times cm$$

2.10. Hair dyeing with i-melanin and colorimetric analysis

I-melanin is dispersed at a concentration of 0.75 mg/mL in distilled water (D·W). A 1 cm × 2 cm bleached hair sample is then immersed in 8 mL of the i-melanin dispersion and shaken at 37 °C for 2 h. After confirming the dyeing effect, the sample is rinsed under running water and towel-dried, repeating this process 5 times to assess color fastness. To examine the effects of different solvents, mordants, and dyeing times on i-melanin, the following experiment was conducted. I-melanin was dispersed at a concentration of 0.5 mg/mL in each of the following solutions: distilled water (D.W), 10 mM NaOH, and 10 mM $CuSO_4$•15 mM H_2O_2 solution. Then 0.5 cm × 0.5 cm bleached hair samples were then immersed in each solution and shaken for 10 min, 20 min, 30 min, 1 h, and 2 h.

The color difference was measured using a colorimeter (JZ-600 instrument; Shenzhen Kingwell Instrument Co., Ltd., Guangdong, China) and analyzed using color analysis management software. The color differences were measured using color meter units of $\Delta E_{ab} = [(\Delta L^*)^2 + (\Delta a^*)^2 + (\Delta b^*)^2]^{½}$, where L* is the brightness; and a* value closer to positive indicates that the sample is more red, and closer to negative indicates more green; for b*, a value closer to positive indicates more yellow, and closer to negative indicates more blue [30].

2.11. Preparation of i-melanin/ZnO composite

A 0.1 g/mL Zinc Chloride solution is prepared in 10 mL. Simultaneously, 1 mg, 10 mg, and 100 mg of i-melanin are each dissolved in a 1 M NaOH solution. Using a burette, the i-melanin NaOH mixture is added dropwise into the 0.1 g/mL Zinc Chloride solution under magnetic stirring. After the reaction is complete, the mixture is centrifuged at 8000 rpm for 5 min. The resulting powder is then washed twice with distilled water and dried in a 60 °C oven.

2.12. Determination of in vitro SPF with i-melanin sunscreen cream

To prepare i-melanin sunscreen, NIVEA® cream (a highly efficient moisturizer with no UV protection properties) was used as the base cream. Pyomelanin was synthesized based on the paper reported previously [9]. For a 5 % cream formulation, 47.5 mg of the base cream was mixed with 2.5 mg of each i-melanin-ZnO variant at concentrations of 0.1 %, 1 %, and 10 %. For a 10 % cream formulation, 45 mg of the base cream was mixed with 5 mg of each i-melanin-ZnO variant at concentrations of 0.1 %, 1 %, and 10 %. In vitro SPF test was conducted using the Diffey and Robson method. A 2 mm-thick quartz glass plate was covered with a 12.5 cm^2 piece of 3 M Transpore™ tape. Then, the prepared i-melanin sunscreen was evenly distributed on the surface using bare finger at a concentration of 2 mg/cm^2. After drying for 20 min in a dark room, a Spectrophotometer U-3900 (HITACHI) was used to measure transmittance from 290 nm to 400 nm in 1 nm increments. Spectral transmittance was measured at three different positions on each sample, and the average value was used for SPF calculation. SPF calculation was calculated as follows.

$$SPF = \frac{\int_{\lambda=290}^{\lambda=400} E(\lambda) \bullet S(\lambda) \bullet d\lambda}{\int_{\lambda=290}^{\lambda=400} E(\lambda) \bullet S(\lambda) \bullet T(\lambda) \bullet d\lambda}$$

E (λ): Relative erythemal spectral effectiveness; S (λ): Solar spectral irradiance ($Wm^{-2}nm^{-1}$); T (λ): Spectral transmittance of the sample (as measured on the U-3900)

3. Results and discussion

3.1. Conversion of 5-hydroxyindole by consecutive FMO monooxygenase and MelC tyrosinase enzyme reaction

In eumelanin biosynthesis, tyrosine serves as the substrate and is enzymatically converted into dopaquinone by tyrosinase. This process initiates the polymerization of radical monomers with similar structures, ultimately leading to eumelanin formation. In contrast, indigo biosynthesis begins with tryptophan, which undergoes hydroxylation at the C3 position, generating a radical at C2, followed by radical-induced dimerization. Notably, significant structural similarities exist between the biosynthetic pathways of melanin pigments and indigo dye.

Building on these biosynthetic principles, this study employed 5-hydroxyindole as a substrate for C3 hydroxylation, followed by a tyrosinase-mediated oxidation reaction. Initially, 5-hydroxyindole was converted into 3,5-dihydroxyindole (DHI) via an FMO enzyme-catalyzed reaction. Sequential oxidation of this intermediate led to the formation of 5,5′-dihydroxyindigo (DHI). Further oxidation by MelC tyrosinase yielded 5,5′,6,6′-tetrahydroxyindigo (THI) and 5,5′,6,6′-tetraquinoneindigo (TQI). This approach successfully synthesized indigo melanin (i-melanin), a novel pigment that integrates the horizontal dimeric structure of indigo with the vertical polymeric configuration characteristic of melanin (Fig. 1A).

3.2. Construction of 5-hydroxyindole conversion host and i-melanin production

Since intracellular indole can be reversibly converted back to

Table 1
Solvent screening for solubilization i-melanin.

Solvent	i-melanin
Acetone	–
Chloroform	+
Methanol	+
Ethanol	+
1 M $NaHCO_3$	+
1 M Na_2CO_3	+
0.1 M NaOH	+++
50 mM NaOH	+++
10 mM NaOH	+++
Ethyl acetate	–
Dimethyl sulfoxide	+++
Distilled water	–

tryptophan by the enzyme tryptophanase (TnaA), an *Escherichia coli* strain lacking the tnaA gene was engineered for i-melanin production. This recombinant strain was transformed with a plasmid co-expressing FMO and MelC, ensuring a dedicated pathway for i-melanin biosynthesis. Following IPTG induction, SDS-PAGE analysis confirmed the simultaneous expression of both enzymes at expected molecular sizes (Fig. 1B).

To evaluate i-melanin production efficiency, various concentrations of 5-hydroxyindole (1–20 mM) were tested. The results showed a positive correlation between substrate concentration and i-melanin yield (Fig. 1C). At 20 mM, approximately 31.3 mg of i-melanin was produced in a 50 mL culture (~626 mg/L). Due to the complex polymeric nature of melanin, conversion rates were assessed based on absolute yield. The highest efficiency (4.3 mg melanin/mg substrate) was observed at 1 mM, while yields declined with increasing substrate concentrations, reaching 3.2 mg/mg at 10 mM and 2.4 mg/mg at 20 mM. Given the solubility of 5-hydroxyindole under ambient conditions (~38 g/L or ~ 285.4 mM), i-melanin production could potentially be scaled to gram-level yields under optimal conditions.

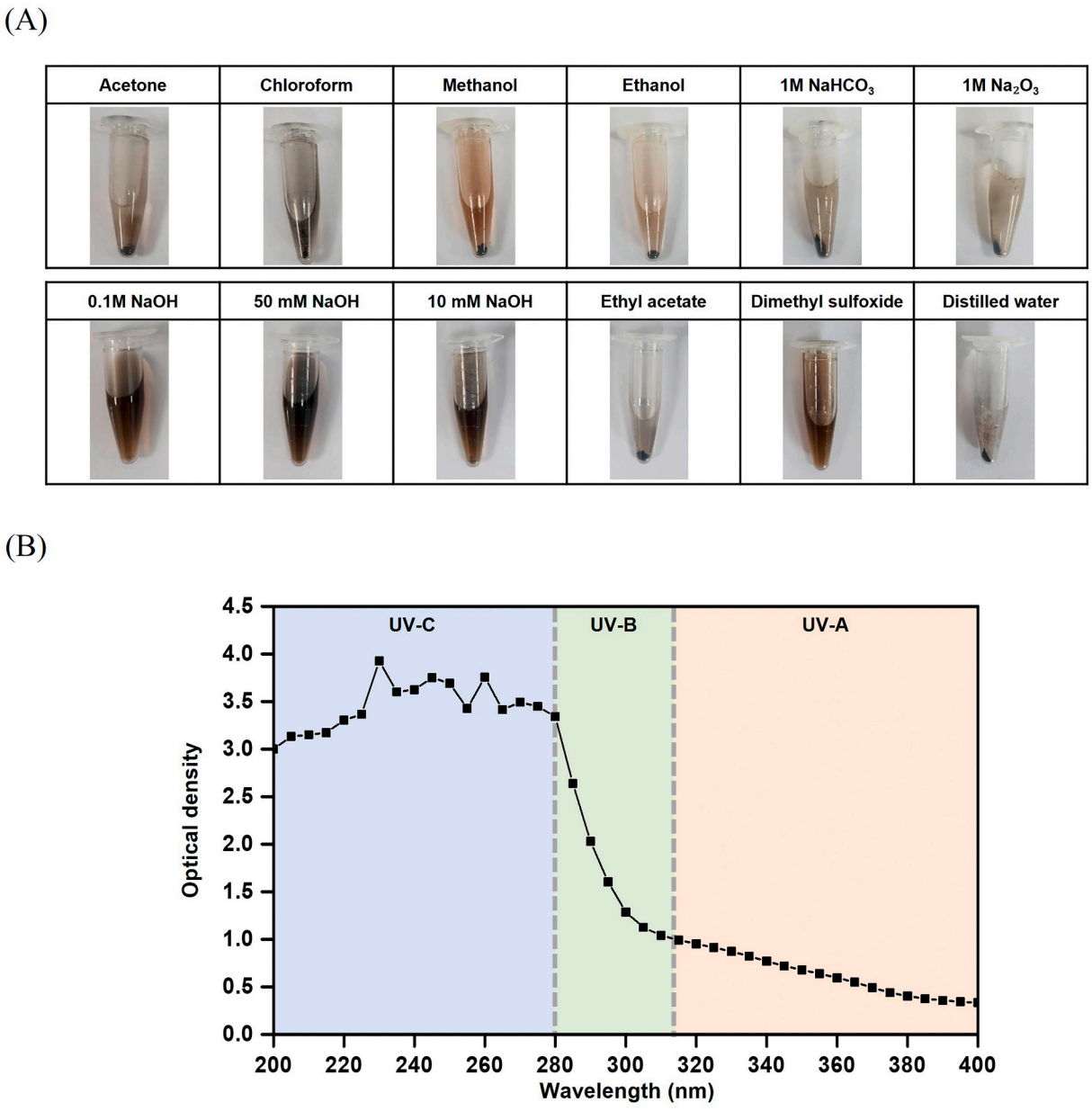

Fig. 2. (A) Screening of solvents for i-melanin solubilization. (B) UV–Vis spectral features of i-melanin across the UV-C to UV-A range.

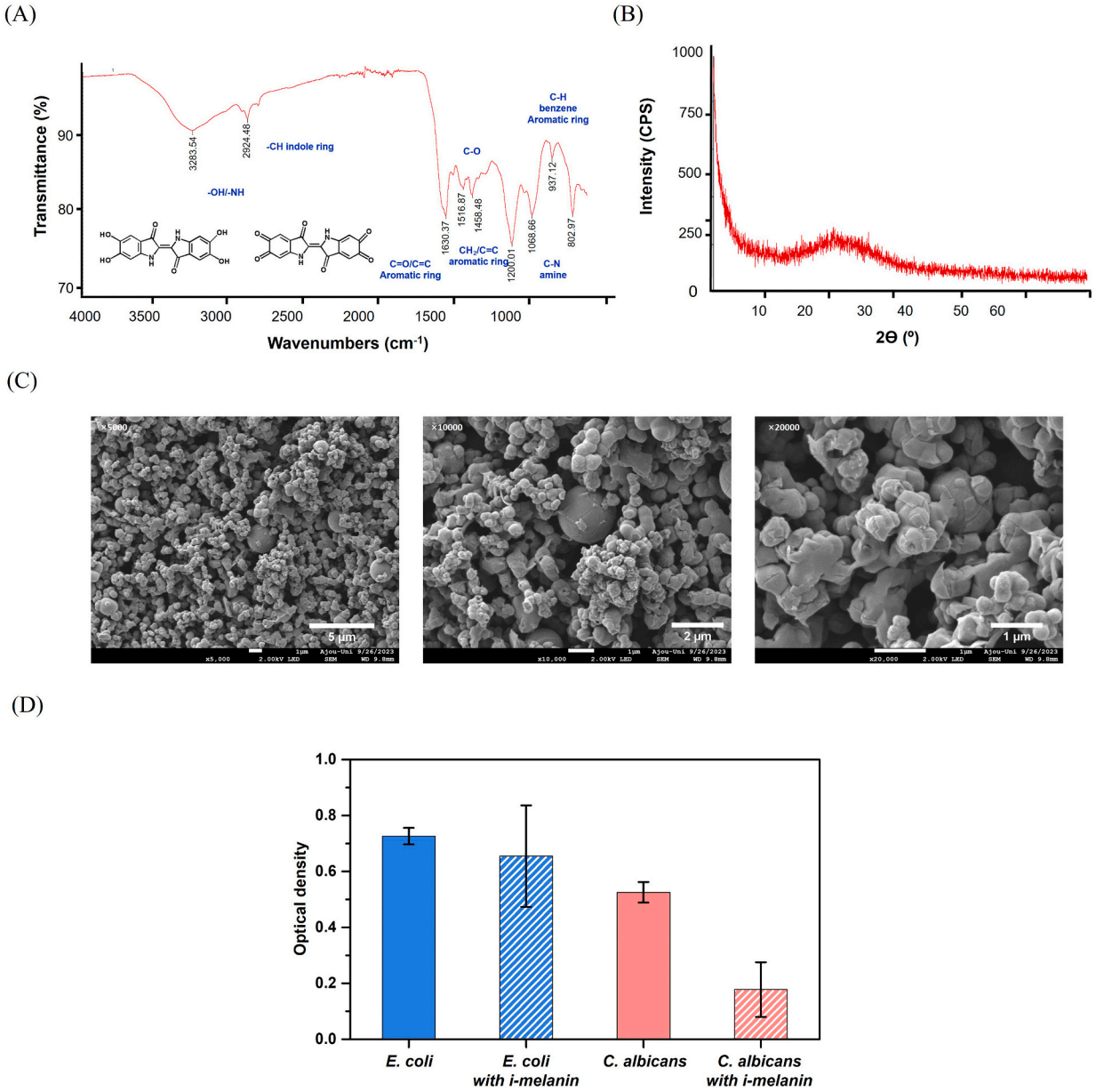

Fig. 3. Structural and physical properties of i-melanin. (A) FT-IR, (B) XRD, and (C) SEM analysis of i-melanin.\ (D) Antibacterial activity of i-melanin against *Escherichia coli* (Gram-negative) and *Candida albicans* (Gram-positive). Growth inhibition was measured by optical density in the presence or absence of i-melanin.

3.3. Solvent screening for i-melanin solubilization

Melanin pigments are generally characterized by poor water solubility, which poses a challenge for practical applications. Therefore, selecting an appropriate solvent to enhance solubility is critical. In this study, i-melanin solubility was tested in 12 different solvents, including acetone, chloroform, methanol, ethanol, $NaHCO_3$, Na_2CO_3, NaOH, ethyl acetate, dimethyl sulfoxide (DMSO), and distilled water (Table 1).

No solubility was observed in water, where i-melanin formed a black precipitate at the bottom of the container. Similarly, minimal solubility was noted in acetone, methanol, ethanol, 1 M $NaHCO_3$, 1 M Na_2CO_3, and ethyl acetate, with visible precipitate formation (Fig. 2A). A slight color shift from black to brown suggested limited dissolution in methanol and ethanol.

Among the tested solvents, NaOH yielded the highest solubility, with optimal dissolution observed at 50 mM. Partial solubility was also achieved in DMSO and chloroform. The solubility profile of i-melanin closely resembled that of eumelanin, indicating similar solvent specificity. For practical applications, optimizing solubility conditions—such as using 50 mM NaOH or employing solubilizing agents—may enhance i-melanin's usability in various formulations. In addition, i-melanin showed good stability in both DMSO and 10 mM NaOH over 5 days at room temperature, indicating that its solubility was not accompanied by degradation. (Fig. S1)

3.4. Spectral features of i-melanin

Unlike traditional eumelanin, i-melanin exhibits a fully black coloration. To characterize its optical properties, absorbance analysis was conducted across wavelengths ranging from 200 to 800 nm. (Fig. S2) The maximum absorbance was recorded at 230 nm, with additional notable absorbance between 250 and 300 nm. In contrast to conventional melanin, which typically displays a broad and gradual decrease in absorbance from 300 to 800 nm, i-melanin exhibited a sharp decline beyond 300 nm (Fig. 2B). This distinct absorbance profile suggests unique optical properties, differentiating i-melanin from

previously reported melanins.

3.5. Structural features of i-melanin FT-IR and MALDI-TOF analysis

To investigate the structure of the newly synthesized i-melanin, analytical techniques, including mass spectrometry of Fourier-transform infrared (FT-IR) and SEM spectroscopy were employed. Due to the complex structure and high molecular weight characteristic of melanin resulting from random polymerization, it was anticipated that separation and analysis of the polymeric form would be challenging. FT-IR spectroscopy was performed to investigate the chemical bonding and functional groups present in i-melanin. The FT-IR spectra obtained for i-melanin are presented in Fig. 3A. Compared to the FT-IR spectra of eumelanin, which shows distinct peaks at 1630 cm^{-1} for C═O stretching and between 1516 and 1458 cm^{-1} for C═C and COO^- stretching in aromatic groups, i-melanin exhibited unique peaks. Specifically, several peaks around 2924.35 cm^{-1} were observed, corresponding to indole C—H groups in indole-ring. And a weak but obviosu broad band around 3283 cm^{-1} was attributed to the presence of O—H and N—H functional groups from indole-ring and 5-hydroxy group. Multiple peaks were observed below 1200 cm^{-1}; however, identification and assignment of these peaks to specific bonds were unclear. To gain further structural insights into i-melanin, additional analyses were conducted.

MALDI-TOF analysis was expected to detect various forms of melanin monomers and oligomers, as the high-energy laser input may fragment the melanin polymer structure. The MALDI-TOF analysis identified major peaks at 393.1 and 264.1 *m/z*, along with additional peaks above 500 m/z, specifically at 524.1, 576.2, 644.1, 711.1, 765.1, 826.0, 863.7, 913.2, and 968.6 m/z. The 644.1 m/z peak likely corresponds to an oligomeric form of i-melanin, specifically a TQI-THI dimer (Fig. S3). However, the precise identification and interpretation of various i-melanin oligomer masses remain challenging due to random radical polymerization [12,40]. Given that diverse structures are generated intracellularly during melanin biosynthesis and may contribute to melanin polymerization, further elucidation of these structures will require integration of NMR analysis with mass spectrometry data. Despite these efforts, the exact structural determination of melanin molecules remains complex and challenging, necessitating ongoing research to achieve a comprehensive understanding [12,40].

3.6. Physical and surface properties of i-melanin; XRD, SEM and TGA analysis

XRD analysis revealed the typical amorphous nature of i-melanin (Fig. 3B), characterized by broad peaks and a weak shoulder peak around $2\theta \approx 20°$, indicating the absence of a well-defined structure. It is widely recognized that various types of melanin generally lack a distinct structure due to the complexities of radical polymerization reactions

The surface morphology of i-melanin was examined using scanning electron microscopy (SEM) at magnifications of 5000×, 10,000×, and 20,000× (Fig. 3C). SEM analysis indicated that i-melanin consists of amorphous material composed of irregularly aggregated particles, consistent with previously reported melanin structures. Notably, i-melanin exhibited tightly packed spherical particles, distinct from the individual, loosely aggregated particles typically observed in eumelanin.

To further evaluate its thermal stability, thermogravimetric analysis (TGA) was conducted on i-melanin up to 1000 °C (Fig. S4). The TGA profile showed weight retention of 48.3 % at 800 °C and 24.0 % at 1000 °C, with phase transitions marked by a steady weight loss beginning around 450 °C and a minor shoulder peak near 250 °C. This thermal resilience may be attributed to its densely packed and stable intracellular structure. Such exceptional thermostability positions i-melanin as a promising material for applications in electronics, solar technology, and other fields requiring high durability and heat resistance.

Table 2
Radical scavenging capacity of i-melanin and comparison with other melanin reported previously.

ABTS	F/*E*-melanin	Tyr-melanin	Sglu-melanin	GA melanin	i-melanin
IC_{50} (mg/mL)	0.27 ± 0.03	0.28 ± 0.15	0.46 ± 0.30	0.07 ± 0.01	0.03 ± 0.01
References	[3]	[13]	[13]	[19]	This study

3.7. Biological activity of i-melanin; growth inhibition against E. coli and C. albicans

The antioxidant capacity of i-melanin was evaluated using the ABTS radical scavenging assay, revealing significantly higher activity compared to previously reported melanins (Table 2). For various melanin types—including eumelanin derived from L-tyrosine (Tyr-melanin), allomelanin from caffeic acid (F/*E*-melanin), naturally occurring melanin in wild-type strains (Sglu-melanin), and gallic acid-based melanin (GA-melanin)—the IC_{50} values were consistently no less than 0.07 ± 0.01 mg/mL, with GA-melanin exhibiting the lowest reported value [3,5,9,12,13,18]. In contrast, i-melanin displayed an IC_{50} of 0.03 ± 0.01 mg/mL, reflecting a nearly 153 % increase in antioxidant capacity compared to Sglu-melanin [5,7]. This enhanced activity may be attributed to its dimeric structure, formed via the FMO enzyme when 5-hydroxyindole is used as a substrate. The symmetrical configuration likely facilitates a more ordered arrangement of i-melanin, contributing to its strong radical-scavenging properties.

The antibacterial activity of i-melanin was assessed against *E. coli* and *C. albicans* strains. At a concentration of 1 mg/mL, i-melanin inhibited *E. coli* growth by approximately 9.8 % and *C. albicans* growth by 66.1 % (Fig. 3D). Notably, i-melanin exhibited stronger inhibitory effects against the gram-positive fungal strain compared to the gram-negative bacterial strain. This inhibitory activity was significantly higher than that of GA-melanin, which our group previously reported to inhibit *E. coli* and *C. albicans* by 4.6 % and 35.2 %, respectively [19]. This increased antimicrobial effect may be attributed to i-melanin's multi-hydroxylated structure and well-ordered molecular arrangement, enhancing its interactions with microbial cell membranes.

3.8. Functional application of i-melanin as a hair dyeing material

The first application of i-melanin has been as a material for hair dyeing. Melanin pigments are generally known for their role in skin and hair pigmentation. As people age, the melanin pigment in hair diminishes, leading to the natural occurrence of gray hair. To introduce melanin pigments into the cuticle layer of hair, the cuticle must be penetrated; thus, melanin can be adsorbed onto the outer cuticle layer to achieve temporary or semi-permanent coloring. For permanent coloring, oxidative dyes are required, but certain components in commercial dyes, such as *p*-phenylenediamine (PPD), are known to cause allergic contact dermatitis. Other diamine-based compounds are sometimes used as PPD alternatives. Furthermore, as the typical process involves bleaching existing melanin pigments followed by oxidative dyeing, unavoidable hair damage often occurs.

In this hair-dyeing study, a method based on the physical penetration of i-melanin pigment for semi-permanent coloring was employed. Commercial bleached hair samples, which were already devoid of melanin pigment, were purchased and used. An i-melanin NaOH aqueous solution at a concentration of 1 mg/L per 10 g of hair was prepared, and the hair was treated with this solution for 1 h, followed by rinsing with water at least twice. After dyeing, a noticeable color change was observed in the hair compared to its pre-dyeing state (Fig. 4A). Compared to control hair samples, i-melanin-dyed hair showed a brightness reduction of over sevenfold and exhibited approximately five

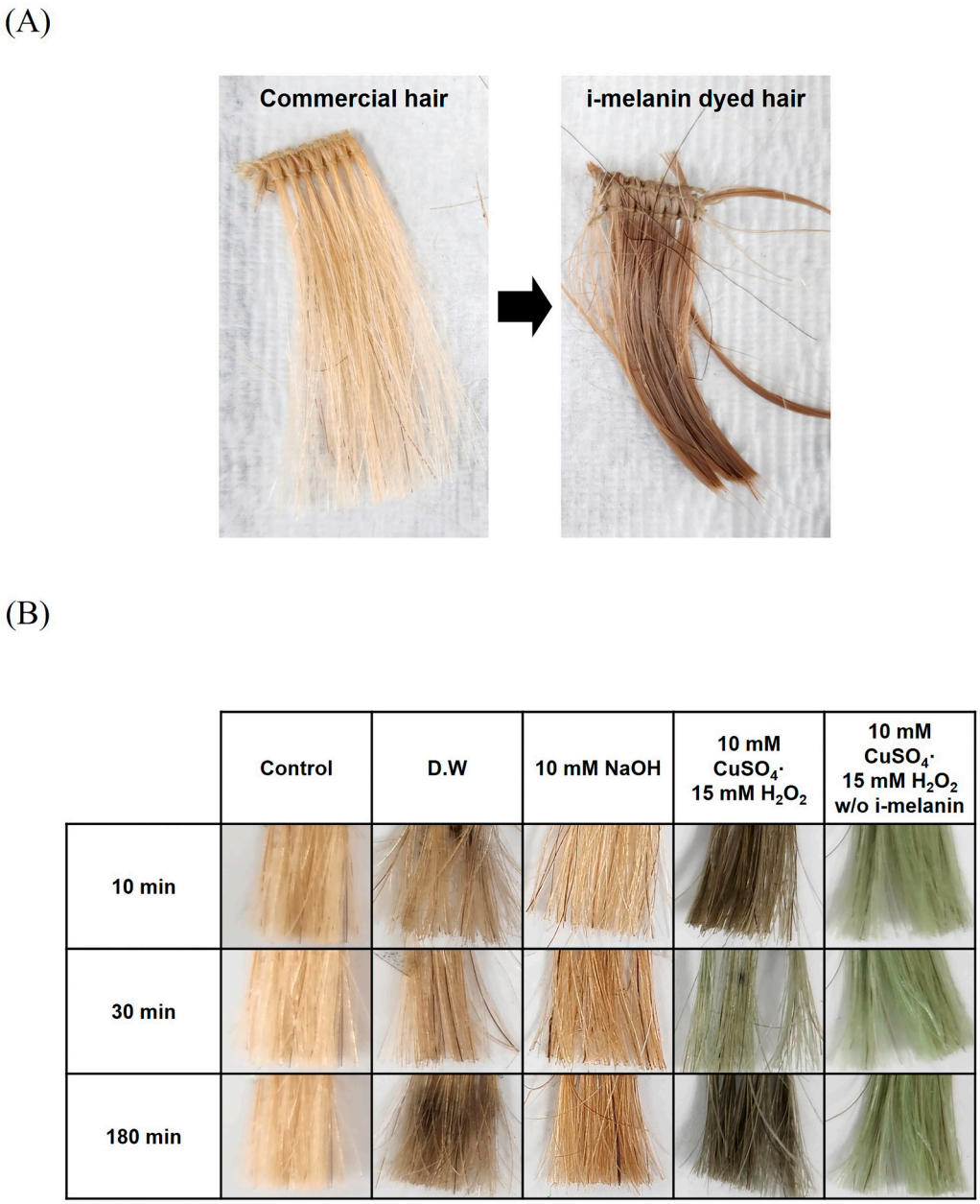

Fig. 4. (A) Hair-dyeing capacity of i-melanin, shown on commercial hair before (left) and after dyeing. (B) Optimization of dyeing conditions, including solvent selection, mordant treatment, and incubation time.

Table 3
Quantitative data for i-melanin incorporated hair from colorimetric analysis.

Samples	L[1]	A[2]	B[3]	ΔE*
Control hair	83.81	3.64	18.77	85.96
i-melanin hair	11.82	8.63	9.17	17.27

L[1]; brightness, a[2]; the closer to +, the redder, the closer to -, the greener; b[3]; the closer to +, the yellower, the closer to -, the bluer. $\Delta E^*_{ab} = [(\Delta L^*)^2 + (\Delta a^*)^2 + (\Delta b^*)^2]^{1/2}$.

times darker coloration overall (Table 3).

To enhance dyeing efficiency, solvents for dissolving extracted i-melanin and oxidative dyeing using $CuSO_4$ and H_2O_2 were tested. When selecting the dyeing solvent, water-based dyeing was found to increase dyeing efficiency over 10 mM NaOH treatment, as observed in the control hair (Fig. 4B). This result suggests that, in water, i-melanin may be better adsorbed to hair through electrostatic attraction when it is ionized, rather than when dissolved in an alkaline solvent. However, when $CuSO_4$ and H_2O_2 mordants were applied, dyeing efficiency decreased due to the degradation of i-melanin itself or coloration from Cu ions.

The results of the hair dyeing test with i-melanin demonstrated that semi-permanent coloring persisted even after washing with water and detergent. It is expected that i-melanin could be applied as a hair dye material without the use of toxic substances that can cause dermatitis, making it suitable for long-term use. Additionally, i-melanin shows high potential for application as a shampoo additive. To fully assess its practicality, however, further studies are needed to evaluate the long-term color stability, washing resistance, and potential effects under various environmental conditions as the melanin was adsorbed onto the surface of the hair without disrupting the cuticle layer.

Enzyme-mediated synthesis, particularly involving tyrosinase MelC enzyme, promotes the formation of melanin-like polymers through the

(A)

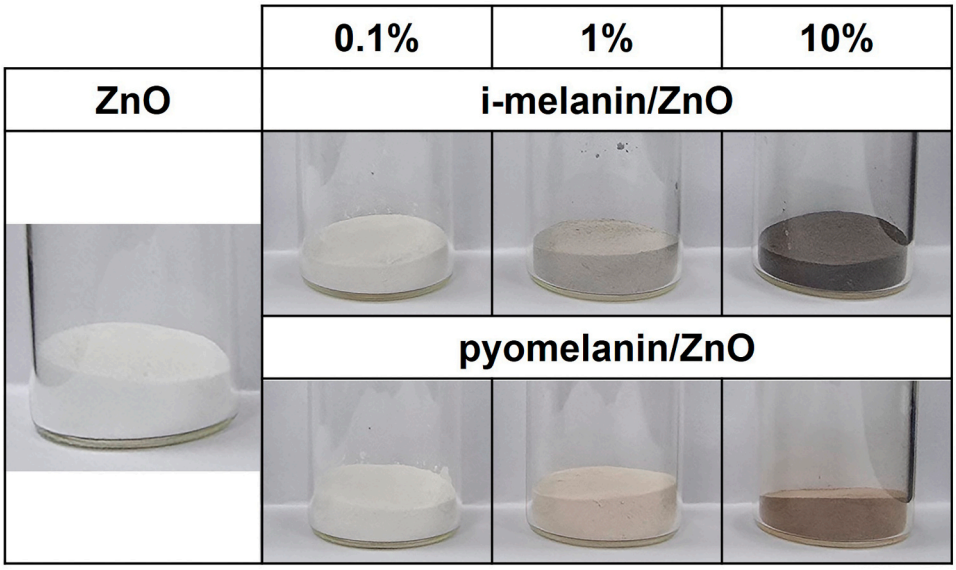

(B)

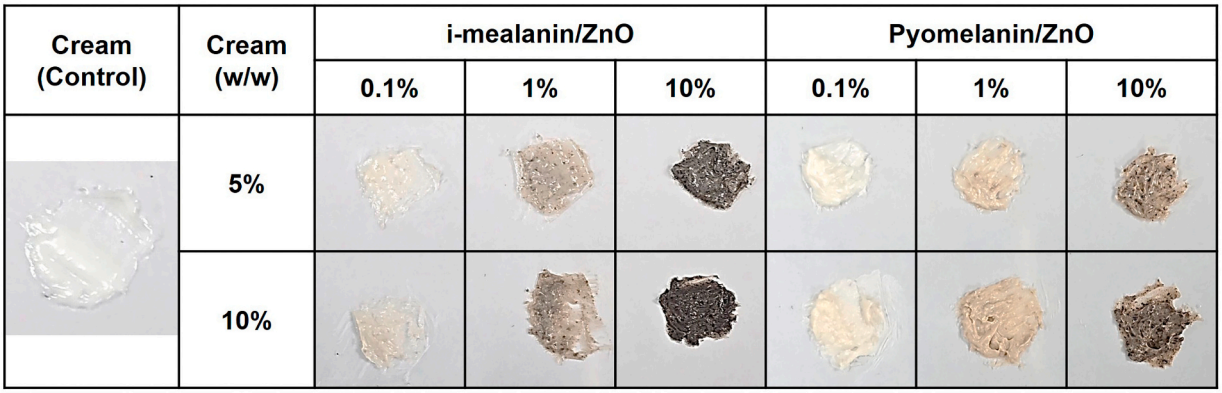

(C)

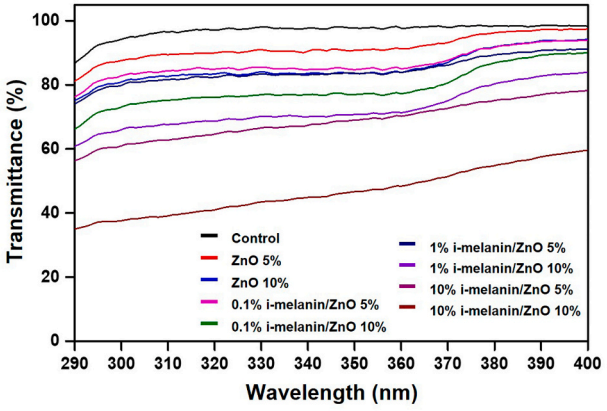

(D)

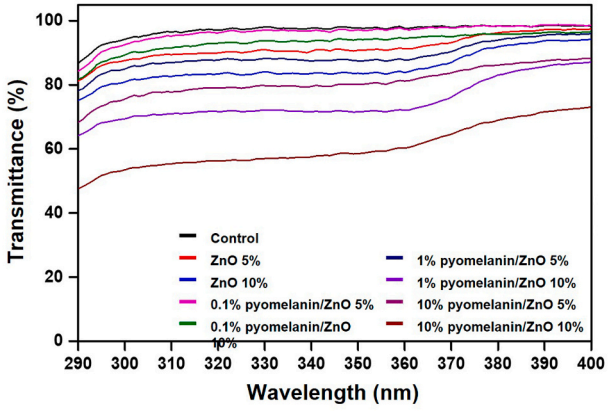

Fig. 5. (A) Complex formation between i-melanin and ZnO at i-melanin concentrations of 0.1 %, 1 %, and 10 %, with a pyomelanin/ZnO complex provided as a control. (B) Sunscreen formulations containing i-melanin/ZnO or pyomelanin/ZnO at 5 % and 10 % concentrations. (C) UV light transmittance (290–400 nm) of i-melanin/ZnO cream at different concentrations. (D) UV light transmittance (290–400 nm) of pyomelanin/ZnO cream at varying concentrations.

Table 4
Determination of sun protection factor (SPF) values and comparion with pyomelanin.

Melanin-ZnO	SPF values	
	5 % Cream (*w*/w)	10 % Cream (w/w)
Control cream	1.04 ± 0.01	–
ZnO	1.12 ± 0.03	1.25 ± 0.03
0.1 % pyomelanin-ZnO	1.05 ± 0.01	1.09 ± 0.00
1 % pyomelanin-ZnO	1.15 ± 0.05	1.41 ± 0.08
0.1 % i-melanin-ZnO	1.19 ± 0.04	1.33 ± 0.03
1 % i-melanin -ZnO	1.23 ± 0.05	1.48 ± 0.05
10 % i-melanin -ZnO	1.58 ± 0.00	2.52 ± 0.11

oxidation of phenolic radical monomners. This process preserves hydroxyl groups, which contribute to antioxidant properties. According to the recently published paper, the degree of oxidation, however, critically affects the development of chromophoric structures that determine color intensity materials [14–16]. Incomplete oxidation can result in melanin complex with fewer conjugated double bonds, leading to lighter pigmentation which is not proper hair dying.

3.9. Functional application of i-melanin as UV-protective cosmetics

The next application of i-melanin is as a UV-protective material for sunscreen formulations. Melanin pigment is well known for its role in protecting human skin from UV radiation. To utilize melanin as a UV-blocking material, it was functionalized with ZnO and formulated into a sunscreen. ZnO, in the form of a white powder, is an inorganic UV-blocking agent recognized for its safety and efficacy by the U.S. Food and Drug Administration (FDA) and is known for its ability to block UVA radiation. It is widely used as an additive in various products. Functionalizing ZnO with melanin offers the advantage of enhancing ZnO's photostability. ZnO, when exposed to UV radiation for prolonged periods, may penetrate dermal cells, potentially causing cytotoxicity. However, when combined with i-melanin, both photostability and the reduction of cellular penetration are improved, thereby lowering toxicity.

First, control ZnO powder and three types of melanin—eumelanin, pyomelanin, and i-melanin—were functionalized with ZnO and prepared as powder materials (Fig. 5A). To observe color changes, i-melanin and pyomelanin were added to ZnO in concentrations of 0.1 %, 1 %, and 10 %. Pure ZnO powder exhibited a white color, while eumelanin- and pyomelanin-functionalized ZnO showed a grayish color. At a 0.1 % concentration, no significant color change in ZnO was observed, but at 1 %, a grayish color appeared, and at 10 % or higher, a black color was observed. When functionalized with 10 % i-melanin, the material appeared completely black. These i-melanin/ZnO and pyomelanin/ZnO materials were then formulated into skin cream at concentrations of 5 % and 10 % (Fig. 5B). The creams were prepared by homogenizing the melanin/ZnO materials at 0.1 %, 1 %, and 10 % concentrations using a homogenizer. No significant color difference was observed between the creams with 5 % and 10 % melanin concentrations, but the original melanin colors were maintained. The color of melanin was more distinct at the 10 % concentration.

The sun protection factor (SPF) of each formulated cream was measured. For each concentration of 5 % and 10 % cream, both pyomelanin and i-melanin samples were evaluated, and SPF values increased with the ZnO concentration in the cream. i-Melanin showed SPF values that were 5–10 % higher than control ZnO even at a 0.1 % concentration, and at 10 %, i-melanin exhibited more than twice the SPF value in the 10 % cream compared to the control (Table 4). Consequently, all sunscreen creams prepared with i-melanin/ZnO materials at a 0.1 % concentration demonstrated higher SPF values than those formulated with ZnO alone. In this experiment, SPF values were lower than the typical SPF range due to the specific methods used for SPF determination. However, the relative SPF values, compared to control cream and ZnO, confirmed the effect of melanin. At a 0.1 % concentration, i-melanin did not cause significant color changes in cream formulation, remaining closer to a natural skin tone, suggesting its potential for use as a UV-protective material. According to recent reports on the application of microbially derived melanin, a cream blended with 5 % fungal melanin exhibited a maximum SPF value of 2.5 [39]. This value was comparable to the SPF values observed for creams blended with 1–5 % i-melanin. In the long term, to utilize melanin as a UV-protective material by forming a complex with metal oxides such as ZnO, various hurdles must be overcome. In the case of melanin, due to its black coloration, it is necessary to enhance the quality of the color when applying it to cosmetic materials. Additionally, the metal oxide used must ensure skin safety and human application safety. Furthermore, when exposed to the environment, considerations regarding environmental safety and potential risks are also essential.

4. Conclusion

In this study, i-melanin was synthesized using 5-hydroxyindole as a substrate through sequential enzymatic reactions catalyzed by flavin-containing monooxygenase (FMO) for C3-specific hydroxylation and MelC tyrosinase for C6-specific hydroxylation and oxidation. The resulting i-melanin exhibited distinct structural and biological properties compared to previously reported eumelanin, pyomelanin, and gallic acid (GA) melanin. Notably, i-melanin displayed a near-black coloration, distinguishing it from conventional melanins, and demonstrated remarkable thermal stability. Solubility tests revealed that NaOH was the most effective solvent, whereas i-melanin remained insoluble in water.

Leveraging these unique properties, the potential application of i-melanin as a semi-permanent hair dye was evaluated. In water-based dyeing tests, i-melanin exhibited high color fastness and excellent hair-dyeing efficiency. Furthermore, to assess its UV-protective potential, an i-melanin/ZnO composite was prepared and incorporated into a commercial cream for sun protection factor (SPF) testing. The i-melanin/ZnO composite achieved SPF values more than twice those of ZnO alone while maintaining a lighter coloration at a 0.1 % i-melanin concentration, making it suitable for cosmetic formulations.

In conclusion, this study successfully biosynthesized a melanin complex inspired by the symmetric dimer structure of indigo dye, yielding a stable and likely planar melanin polymer structure due to its symmetric conformation. This structural stability appears to contribute to the high thermal resilience and biological activity of i-melanin. Given its scalable production, i-melanin holds significant potential as a functional ingredient in cosmetic applications, particularly for UV protection and durable coloration.

CRediT authorship contribution statement

Chan-Seo Yeo: Writing – original draft, Investigation. **Jongyun Choi:** Writing – original draft, Investigation. **Hee-Jung Kim:** Writing – original draft, Investigation. **Joo Hee Chung:** Investigation. **HyunA Park:** Writing – original draft, Investigation, Conceptualization. **Jong-Bok Seo:** Investigation, Conceptualization. **Ji Chul Jung:** Writing – original draft, Investigation, Conceptualization. **Wonjong Jung:** Writing – original draft, Investigation, Conceptualization. **Kwon-Young Choi:** Writing – review & editing, Writing – original draft, Methodology, Investigation, Conceptualization.

Declaration of competing interest

The authors declare that the research was conducted in the absence of any commercial or financial relationships that could be construed as potential conflicts of interest.

Acknowledgements

This work was supported by the National Research Foundation (NRF) of Korea grant funded by the Ministry of Education, Science, and Technology (MEST) [2021R1A2C1007519] and the R&D Program of MOTIE/KEIT [grant numbers: 20025698 and 20018132].

Appendix A. Supplementary data

Supplementary data to this article can be found online at https://doi.org/10.1016/j.porgcoat.2025.109368.

Data availability

Data will be made available on request.

References

[1] A.N. Tran-Ly, C. Reyes, F. Schwarze, J. Ribera, Microbial production of melanin and its various applications, World J. Microbiol. Biotechnol. 36 (2020) 170.
[2] S. Park, C. Lee, J. Lee, S. Jung, K.-Y. Choi, Applications of natural and synthetic Melanins as biosorbents and adhesive coatings, Biotechnol. Bioprocess Eng. 25 (2020) 646–654.
[3] S. Jang, H. Gang, B.-G. Kim, K.-Y. Choi, FCS and ECH dependent production of phenolic aldehyde and melanin pigment from l-tyrosine in Escherichia coli, Enzyme Microb Tech 112 (2018) 59–64.
[4] S. Singh, S.B. Nimse, D.E. Mathew, A. Dhimmar, H. Sahastrabudhe, A. Gajjar, V. A. Ghadge, P. Kumar, P.B. Shinde, Microbial melanin: recent advances in biosynthesis, extraction, characterization, and applications, Biotechnol. Adv. 107773 (2021).
[5] S.-Y. Ahn, S. Jang, P.D. Sudheer, K.-Y. Choi, Microbial production of melanin pigments from caffeic acid and L-tyrosine using Streptomyces glaucescens and FCS-ECH-expressing Escherichia coli, Int. J. Mol. Sci. 22 (2021) 2413.
[6] U. Perez-Cuesta, L. Aparicio-Fernandez, X. Guruceaga, L. Martin-Souto, A. Abad-Diaz-de-Cerio, A. Antoran, I. Buldain, F.L. Hernando, A. Ramirez-Garcia, A. Rementeria, Melanin and pyomelanin in Aspergillus fumigatus: from its genetics to host interaction, Int. Microbiol. 23 (2020) 55–63.
[7] S.Y. Ahn, S. Jang, P. Sudheer, K.Y. Choi, Microbial production of melanin pigments from caffeic acid and L-tyrosine using Streptomyces glaucescens and FCS-ECH-expressing Escherichia coli, Int. J. Mol. Sci. 22 (2021).
[8] K.P. Vercruysse, The “unconventional” effect of cysteine on the in vitro synthesis of melanin, ACS Omega 9 (2024) 22794–22800.
[9] D. Seo, K.-Y. Choi, Heterologous production of pyomelanin biopolymer using 4-hydroxyphenylpyruvate dioxygenase isolated from Ralstonia pickettii in Escherichia coli, Biochem. Eng. J. 157 (2020) 107548.
[10] M. Brenner, V.J. Hearing, The protective role of melanin against UV damage in human skin, Photochem. Photobiol. 84 (2008) 539–549.
[11] D. Bajrami, A. Zubiaga, T. Renggli, C. Kirsch, F. Spano, D. Fehr, P. von Schulthess, A. Lindhorst-Peters, S. Huber, E. Roider, R.M. Rossi, A.A. Navarini, M. Bonmarin, Variations of skin thermal diffusivity on different skin regions, Skin Res. Technol. 30 (2024) e13622.
[12] H. Park, I. Yang, M. Choi, K.-S. Jang, J.C. Jung, K.-Y. Choi, Engineering of melanin biopolymer by co-expression of MelC tyrosinase with CYP102G4 monooxygenase: structural composition understanding by 15 tesla FT-ICR MS analysis, Biochem. Eng. J. 157 (2020) 107530.
[13] S.-Y. Ahn, M. Choi, D.-w. Jeong, S. Park, H. Park, K.-S. Jang, K.-Y. Choi, Synthesis and chemical composition analysis of protocatechualdehyde-based novel melanin dye by 15T FT-ICR: high dyeing performance on soft contact lens, Dyes Pigments, 160 (2019) 546–554.
[14] L.Z. Yang, X. K.; Zhang, J. H.; Hu, J. F.; Zhang, T.; Gu, Z. P.; Li, Y. W., Synthetic melanin hair dye., Acta Polym. Sin., 55 (114) 192–201.
[15] T. Zhang, B. Liang, J.-H. Zhang, L. Yang, J.-F. Hu, Y.-W. Li, Sunlight-induced permanent hair dyeing, Chin. J. Polym. Sci. 43 (2025) 261–270.
[16] T. Zhang, J. Hu, L. Guo, Z. Gu, X. Jiang, Y. Li, Nature-inspired safe and efficient hair dyes: beyond the traditional hair dyes, Green Chem. 26 (2024) 3125–3138.
[17] G.S. Kiran, S.A. Jackson, S. Priyadharsini, A.D.W. Dobson, J. Selvin, Synthesis of Nm-PHB (nanomelanin-polyhydroxy butyrate) nanocomposite film and its protective effect against biofilm-forming multi drug resistant Staphylococcus aureus, Sci. Rep. 7 (2017) 9167.
[18] S. Park, Y.-H. Yang, K.-Y. Choi, One-pot production of thermostable PHB biodegradable polymer by co-producing bio-melanin pigment in engineered Escherichia coli, Biomass Convers. Biorefinery (2022). Published online.
[19] S. Park, C.-S. Yeo, W. Jung, K.-Y. Choi, Gallic acid melanin pigment hydrogel as a flexible macromolecule for articular motion sensing, New Biotechnol. 84 (2024) 85–95.
[20] N. Brizuela Guerra, J.V. Morais Lima, N.L. Nozella, M.H. Boratto, J.V. Paulin, C.F. d.O. Graeff, Electrochemical doping effect on the conductivity of melanin-inspired materials, ACS Appl. Bio Mater. 7 (2024) 2186–2196.
[21] S. Ghattavi, A. Homaei, P. Fernandes, Marine natural products for biofouling elimination in marine environments, Biocatal. Agric. Biotechnol. 61 (2024) 103385.
[22] S. Ghattavi, A. Homaei, E. Kamrani, D. Saberi, M. Daliri, Fabrication of antifouling coating based on chitosan-melanin hybrid nanoparticles as sustainable and antimicrobial surface, Prog. Org. Coat. 174 (2023) 107327.
[23] S. Ghattavi, A. Homaei, E. Kamrani, Innovative CuO-melanin hybrid nanoparticles and polytetrafluoroethylene for enhanced antifouling coatings, Colloids Surf. B: Biointerfaces 246 (2025) 114387.
[24] K. Ghattavi, A. Homaei, E. Kamrani, S.-K. Kim, Melanin pigment derived from marine organisms and its industrial applications, Dyes Pigments 201 (2022) 110214.
[25] R. Sarangarajan, S.P. Apte, The polymerization of melanin: a poorly understood phenomenon with egregious biological implications, Melanoma Res. 16 (2006) 3–10.
[26] S. Mondal, A. Thampi, M. Puranik, Kinetics of melanin polymerization during enzymatic and nonenzymatic oxidation, J. Phys. Chem. B 122 (2018) 2047–2063.
[27] Y. Tobimatsu, M. Schuetz, Lignin polymerization: how do plants manage the chemistry so well? Curr. Opin. Biotechnol. 56 (2019) 75–81.
[28] J.C. del Río, J. Rencoret, A. Gutiérrez, T. Elder, H. Kim, J. Ralph, Lignin monomers from beyond the canonical monolignol biosynthetic pathway: another brick in the wall, ACS Sustain. Chem. Eng. 8 (2020) 4997–5012.
[29] H.-R. Jung, T.-R. Choi, Y.H. Han, Y.-L. Park, J.Y. Park, H.-S. Song, S.-Y. Yang, S. K. Bhatia, R. Gurav, H. Park, S. Namgung, K.-Y. Choi, Y.-H. Yang, Production of blue-colored polyhydroxybutyrate (PHB) by one-pot production and coextraction of indigo and PHB from recombinant *Escherichia coli*, Dyes Pigments 173 (2020) 107889.
[30] S. Namgung, H.A. Park, J. Kim, P.-G. Lee, B.-G. Kim, Y.-H. Yang, K.-Y. Choi, Ecofriendly one-pot biosynthesis of indigo derivative dyes using CYP102G4 and PrnA halogenase, Dyes Pigments 162 (2019) 80–88.
[31] H.-J. Kim, S. Jang, J. Kim, Y.-H. Yang, Y.-G. Kim, B.-G. Kim, K.-Y. Choi, Biosynthesis of indigo in *Escherichia coli* expressing self-sufficient CYP102A from *Streptomyces cattleya*, Dyes Pigments 140 (2017) 29–35.
[32] N. Loncar, H.L. van Beek, M.W. Fraaije, Structure-based redesign of a self-sufficient flavin-containing monooxygenase towards indigo production, Int. J. Mol. Sci. 20 (2019).
[33] T. Heine, Indigoid dyes by group E monooxygenases: mechanism and biocatalysis, Turkish journal of biology = Turk biyoloji dergisi 400 (2019) 939–950.
[34] T. Heine, K. Tucker, N. Okonkwo, B. Assefa, C. Conrad, A. Scholtissek, M. Schlomann, G. Gassner, D. Tischler, Engineering styrene monooxygenase for biocatalysis: reductase-epoxidase fusion proteins, Appl. Biochem. Biotechnol. 181 (2017) 1590–1610.
[35] X. Han, W. Wang, X. Xiao, Microbial biosynthesis and biotransformation of indigo and indigo-like pigments, Chin. J. Biotechnol. 24 (2008) 921–926.
[36] F. Li, Q. Chen, H. Deng, S. Ye, R. Chen, J.D. Keasling, X. Luo, One-pot selective biosynthesis of Tyrian purple in Escherichia coli, Metab. Eng. 81 (2024) 100–109.
[37] Y. Yuk, J.-H. Jang, S. Park, H. Park, J.-O. Ahn, Y.-H. Yang, S. Ham, S.-H. Park, K. Park, S.Y. Kim, Y.S. Kim, J. Lee, U.-J. Lee, B.-G. Kim, K.-Y. Choi, Production of bio-indigo dye by surmounting its physical and chemical insoluble nature, Dyes Pigments 218 (2023) 111466.
[38] S. Namgung, H. Park, J. Kim, P.G. Lee, B.G. Kim, Y.H. Yang, K.Y. Choi, Ecofriendly one-pot biosynthesis of indigo derivative dyes using CYP102G4 and PrnA halogenase, Dyes Pigments 162 (2019) 80–88.
[39] J.-J. Oh, J.Y. Kim, S.H. Son, W.-J. Jung, D.H. Kim, J.-W. Seo, G.-H. Kim, Fungal melanin as a biocompatible broad-spectrum sunscreen with high antioxidant activity, RSC Adv. 11 (2021) 19682–19689.
[40] Y. Kim, H. Park, P. Lee, K. Woo, K.Y. Choi, H.H. Lee, Biosynthesis of tyrosine-derived i-melanin and its characteristics for organic thin film transistor device, Mater. Today Adv. 26 (2025) 100582.